Possible One-Dimensional ^{3}He Quantum Fluid Formed in Nanopores

Junko Taniguchi,[1,*] Akira Yamaguchi,[1] Hidehiko Ishimoto,[1] Hiroki Ikegami,[2] Taku Matsushita,[3] Nobuo Wada,[3,†] Silvina M. Gatica,[4] Milton W. Cole,[4] Francesco Ancilotto,[5] Shinji Inagaki,[6] and Yoshiaki Fukushima[6]

[1]*Institute for Solid State Physics, University of Tokyo, 5-1-5 Kashiwanoha, Kashiwa, Chiba 277-8581, Japan*

[2]*Low Temperature Physics Laboratory, Discovery Research Institute, RIKEN (The Institute of Physical and Chemical Research), Hirosawa 2-1, Wako, Saitama 351-0198, Japan*

[3]*Department of Physics, Graduate School of Science, Nagoya University, Chikusa-ku, Nagoya 464-8602, Japan*

[4]*Department of Physics, Pennsylvania State University, University Park, 16802 Pennsylvania, USA*

[5]*INFM–Dipartimento di Fisica, Università di Padova, Via Marzolo 8, I-35131 Padova, Italy*

[6]*Toyota Central R&D Laboratories, Inc., Yokomichi, Nagakute, Aichi 480-1192, Japan*

(Received 31 May 2004; published 14 February 2005)

Heat capacity measurements have been made down to 5 mK for ^{3}He fluid films adsorbed in one-dimensional (1D) nanometer-scale pores, 28 Å in diameter, preplated with ^{4}He of 1.47 atomic layers. At low ^{3}He density, the heat capacity shows a density-dependent, Schottky-like peak near 150 mK asymptoting to the value corresponding to a 2D Boltzmann gas at high temperatures. The peak behavior is attributed to the crossover from a 2D gas to a 1D state at low temperatures. The degenerate state of the 1D ^{3}He fluid is indicated by a predominantly linear temperature dependence below about 30 mK.

DOI: 10.1103/PhysRevLett.94.065301 PACS numbers: 67.55.–s, 67.70.+n, 68.65.–k, 68.90.+g

Helium 3 is an ideal object to study Fermi fluids in three and low dimensions, both experimentally and theoretically [1]. The bulk ^{3}He liquid was recognized to have a strong 3D spin correlation that enhances the P-wave superfluid. The 2D Fermi fluid is known to exist when ^{3}He atoms condense as thin films on flat solid surfaces, e.g., graphite [2], hectorite [3], Cs [4], and the free surface of ^{4}He [5]. The interaction in the ^{3}He films is easily controlled by varying the ^{3}He density, precoating with ^{4}He [6,7], or changing the substrate. An absolute 2D Fermi degeneracy is realized in such films, since all of the atoms are in the ground state for motion perpendicular to the surface, leaving 2D motion along the surface. In contrast with the 3D and 2D Fermi fluids, a degenerate 1D ^{3}He fluid has not yet been realized, to the best of our knowledge, although a 1D ^{4}He fluid has been studied within the 1D pores of FSM-16 possessing a diameter of 18 Å [8]. Manifestly, one way to make a new 1D degenerate ^{3}He fluid is to confine the atoms in very narrow 1D pores. The 1D limit can be achieved when the atoms are in the transverse ground state, occurring when the Fermi energy is lower than the energy gap between the ground state and the first excited state. In this Letter, we describe the realization of this 1D degenerate state of a ^{3}He fluid confined in 1D nanometer-scale pores of FSM-16.

Recent innovations in the synthesis of mesoporous materials whose pore diameters are a few nanometers provide many 1D substrates, e.g., FSM-16, MCM-41, and carbon nanotube bundles [9]. Among these substrates, FSM-16 is chemically and thermally stable and has uniform pores [10]. Furthermore, the pore diameter can be controlled from 15 to 48 Å [11]. Here we used FSM-16 whose pore diameter is 28 Å. This value has an ambiguity of about 2 Å, because no precise size determination method has been established. The material is obtained as a powder whose mean grain size is 3000 Å. Each grain has a regular array of 1D tunnels about 3000 Å in length. The FSM-16 powders were mixed with 0.5 μm silver powders and then sintered on silver disks. They were put into the sample cell for pressure (P) and heat capacity measurements. The adsorption area S in the cell is estimated to be 85 ± 5 m^2 by fitting the N_2 isotherm at 77 K to the Brunauer-Emmett-Teller equation in the P range between 5 and 16 kPa. In the following, the coverage n is described as the amount per unit adsorption area.

In a preliminary study of ^{3}He in the 1D pores 28 Å in diameter [12], the fluid state appears at a certain coverage on the second layer. The adatoms on the first layer form a localized solid. In order to achieve the 1D degenerate fluid, without any contribution from the underlying solid ^{3}He, it is usual to preplate a substrate with ^{4}He. Therefore, it is important to investigate how the adsorbed ^{4}He atoms form layers on the pore walls. For this purpose, the ^{4}He vapor pressure was measured in $0.1 < P < 100$ Pa as a function of the ^{4}He coverage (n_4), where the temperature ranges from 6 to 0.5 K depending on the coverage. The observed pressure provides the chemical potential of the film. In the Frenkel-Halsey-Hill model, the chemical potential on the surface of the ^{4}He film is described as the sum of a van der Waals potential from the substrate and that of the bulk liquid [13]. The dominant first term is written as $-\Gamma/\delta^3$, where δ is the film thickness and Γ is a constant. Then, the film thickness is given by $\delta = [(T/\Gamma)\ln(P_0/P)]^{-1/3}$, where T is the temperature and P_0 is the saturated vapor pressure at T. Assuming the value $\Gamma = 1100$ KÅ^3 of a glass substrate [14], we obtained the coverage n_4 dependence of δ as shown in Fig. 1(a). δ increases almost linearly with n_4

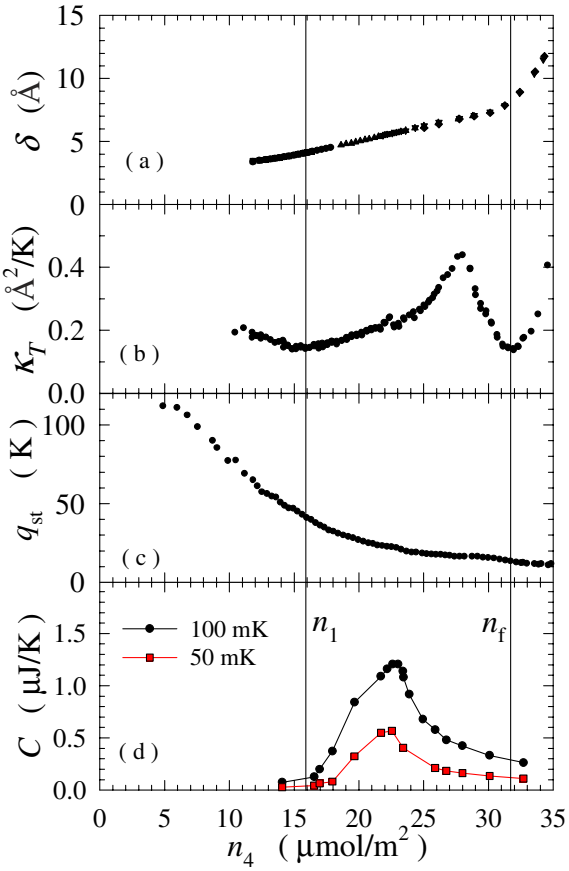

FIG. 1 (color online). Coverage n_4 dependences of (a) film thickness, (b) compressibility of the films, (c) isosteric heat of adsorption, and (d) isotherms of heat capacity for ^{4}He adsorbed in 1D 28 Å pores.

up to the coverage $n_f = 31.8 \pm 1.0$ μmol/m^2, followed by an abrupt increase above n_f. A small deviation from linear dependence is related to the interaction among the adatoms. Figure 1(b) is the coverage dependence of the isothermal compressibility κ_T given by $\kappa_T = S/(n^2RT) \times [\partial \ln P/\partial n]_T^{-1}$, where R is the gas constant. The minimum of κ_T at $n_1 = 15.9 \pm 0.5$ μmol/m^2 corresponds to the first layer completion. The isosteric heat of sorption $q_{st}(T)$ obtained from $q_{st}(T) = -[\partial \ln P/\partial(1/T)]_n$ is given in Fig. 1(c). At the first layer's completion n_1, $q_{st}(T = 3\ \mathrm{K}) = 41$ K. Above n_f, q_{st} approaches 12 K, the value for the bulk ^{4}He liquid at $T = 1$ K. These values in Figs. 1(a)–1(c) agree semiquantitatively with those obtained from a calculation employing a density functional method [15–17]. Thus the ^{4}He coverage dependence can be understood as uniform layer formation on the 1D pore walls up to n_f, just as on planar solid surfaces.

Heat capacity isotherms of ^{4}He are shown in Fig. 1(d). The Bose fluid state is indicated by a characteristic decrease [3,8] above the onset coverage of 22 μmol/m^2. Based on this, the ^{4}He preplating of $n_4 = 23.4$ μmol/m^2 ($1.47n_1$), just above the superfluid onset coverage, was chosen to realize a ^{3}He fluid state. Then the ^{4}He film thickness is estimated to be 5.5 Å from Fig. 1(a). Since the ^{3}He atoms are adsorbed on the ^{4}He film, they are confined in the 1D tube about 17 Å in diameter. The ^{3}He density (n_3) was varied from 0.056 to 0.51 μmol/m^2. The Fermi temperature T_{F1D} as a noninteracting 1D Fermi gas is calculated to be $T_{F1D} = 18$ mK for the lowest coverage density where the mean interparticle separation along the tube is $d_{1D} = 33$ Å.

Using a small $PrNi_5$ demagnetization refrigerator, the sample was cooled to 4 mK, and the heat capacity was measured with an adiabatic heat pulse method. Temperatures were determined with a fast response La-CMN(5%) thermometer between 4 and 50 mK and a Matsushita carbon resistor (ERC-18SG, 50 Ω) above 40 mK. They were calibrated with a ^{3}He melting curve thermometer. At the lowest temperature, the thermal relaxation time was about 10 sec for the La-CMN thermometer itself and less than 20 sec over the sample cell, depending on the magnitude of the heat capacity of the adsorbed ^{4}He and ^{3}He. The relaxation times were sufficiently short for the measurement to be reliable. The ^{3}He heat capacity was obtained by subtracting the contribution from the adsorbed ^{4}He.

Figure 2(a) shows the temperature dependences of the molar ^{3}He heat capacity C/n_3. For all coverages, C/n_3 collapses below about 30 mK, approaching a linear T

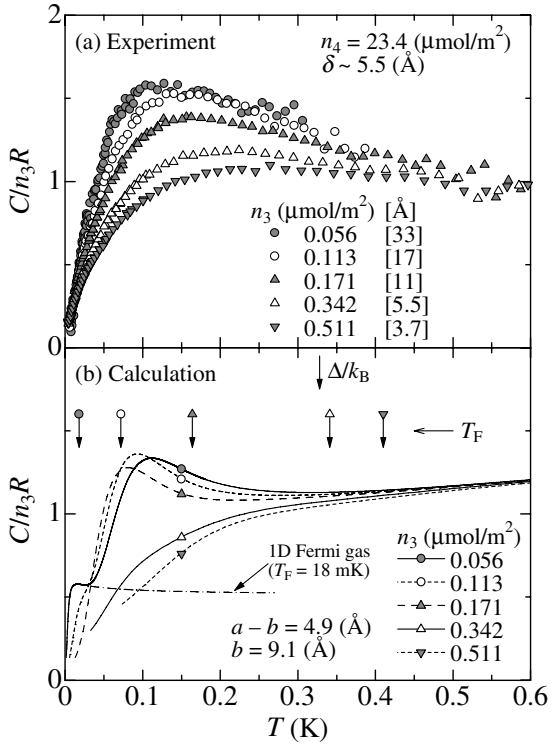

FIG. 2. (a) Molar heat capacities of ^{3}He adsorbed in the ^{4}He preplated 1D pores for various ^{3}He coverages (n_3) and interparticle mean distances (d_{1D}) along the 1D pore. (b) Calculated heat capacities of noninteracting gas in the 1D pore (see the text).

dependence, as described later in detail. With increasing T, the specific heat C/n_3 at the lowest coverage $n_3 = 0.056\ \mu\mathrm{mol/m^2}$ shows a characteristic maximum of $1.5R$ at $T \approx 150$ mK and approaches the value $C/n_3 \approx R$ above about 300 mK. The maximum disappears at high coverages.

In order to explain the observed phenomena, we calculate the eigenstate energies of a ^{3}He atom in the adsorption potential of the 1D nanometer-scale pore and derive the heat capacity of noninteracting ^{3}He gas at densities corresponding to the present experiment.

The substrate potential $U_{\mathrm{subst}}(r)$ is derived in the same way as for the flat surface [14]. It is shown in the inset of Fig. 3, where r is a radius from the center of the pore $2a = 28$ Å in diameter. The potential profile near the pore wall, typically from $0.5a$ to a (7 to 14 Å), is similar to $-\Gamma/(r-a)^3$ of which the power dependence is derived for the flat substrate. In the ^{4}He-preplated pore, the potential $U(r)$ for a ^{3}He atom is shown in the inset of Fig. 3 as the thick solid line, where $U(r) = U_{\mathrm{subst}}(r)$ at $r < b$ and the actual pore radius is reduced to b by the ^{4}He solid layer $(a-b)$ in thickness. The energy levels of the ^{3}He atom in the potential $U(r)$ are shown in Fig. 3, where the differences from the ground state energy, $E_{\ell m} - E_{00}$, are plotted as a function of b. Indices ℓ and m are the quantum numbers of the eigenfunctions about radius r and azimuthal angle, respectively. The states shown with dashed lines ($\ell = 0$) are the 2D states of which each function shows a single probability peak at a radius a little smaller than b. When b is close to a, their energies approach $E_{0m} - E_{00} = \hbar^2/(2m_{^3\mathrm{He}})(m/b)^2$, and the ^{3}He atom is near the pore wall. For a small radius of b, 3D states with $\ell \neq 0$ appear as marked with the solid lines. When the kinetic energy of the ^{3}He atom is much lower than $\Delta = E_{01} - E_{00}$, the azimuthal motion is limited to the circularly symmetric ground state leaving only the free motion along the 1D longitudinal direction. The largest kinetic energy of the 1D ideal Fermi gas, i.e., the Fermi energy, is given as $k_{\mathrm{B}}T_{\mathrm{F1D}} = h^2/(32m_{^3\mathrm{He}}d_{\mathrm{1D}}^2)$. The 1D distance is given by $d_{\mathrm{1D}} = S/(2\pi a n_3 N_{\mathrm{A}})$, where N_{A} is Avogadro's number. Therefore a degenerate 1D Fermi gas is realized at coverages where the 1D Fermi energy $k_{\mathrm{B}}T_{\mathrm{F1D}}$ becomes lower than the gap energy Δ in the cross section and at the temperatures sufficiently lower than $(\Delta/k_{\mathrm{B}} - T_{\mathrm{F1D}})$.

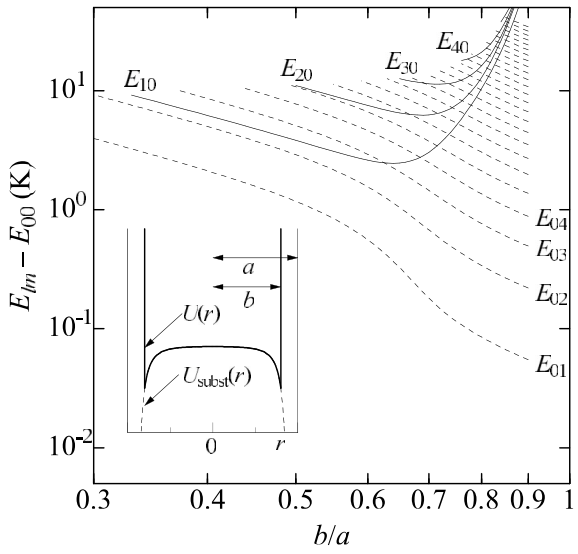

FIG. 3. Eigenstate energies $E_{\ell m} - E_{00}$ of a ^{3}He atom for the azimuthal motion in a potential $U(r)$ as a function of b/a. The inset shows a substrate potential $U_{\mathrm{subst}}(r)$ in the cross section of the 1D pore $a = 14$ Å in radius, and a potential $U(r)$ assumed for a ^{3}He atom in the ^{4}He preplated pore with b in radius and $(a-b)$ in ^{4}He thickness.

In the present experiment, the appropriate radius of the ^{4}He preplated pore is $b = 9.1$ Å, i.e., $b/a = 0.65$, in Fig. 3, which gives the gap energy $\Delta/k_{\mathrm{B}} = 328$ mK. Based on the energy levels at $b/a = 0.65$ in the cross section and a free transverse motion along the pore, we calculated the heat capacities for the noninteracting ^{3}He gas with the five densities as shown in Fig. 2(b), where the Fermi temperature T_{F} at each coverage is indicated by the arrow. Since $T_{\mathrm{F}} = 18$ mK of the lowest density is much lower than $\Delta/k_{\mathrm{B}} = 328$ mK, the calculated C/n_3R (●) exactly agree with that of the 1D Fermi gas below about $0.1 \times \Delta/k_{\mathrm{B}}$ (33 mK). Thus, the calculations for the lowest two coverages, (●) and (○) in Fig. 2(b), satisfy the 1D condition below about 30 mK. With increasing T, the calculated C/n_3R for the lower three coverages in Fig. 2(b) show Schottky peaks at about 100 mK caused by thermal excitation to the first azimuthal excited state of E_{01} state in Fig. 3. At the higher temperatures, excitation to the higher E_{0m} states yields the 2D classical gas heat capacity, $C/n_3R = 1$. The Schottky peak is a characteristic feature revealing a crossover from the 1D low-temperature

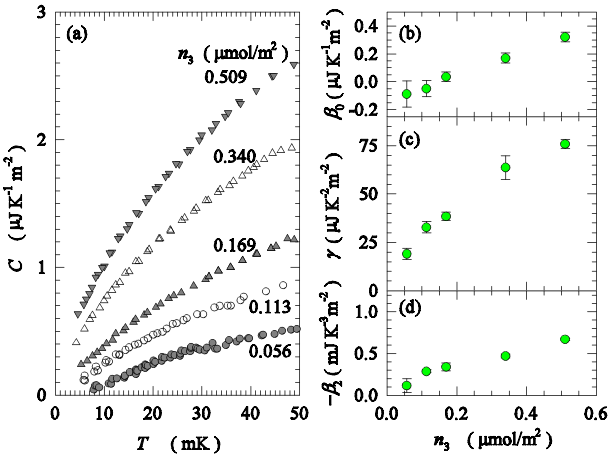

FIG. 4 (color online). (a) Low-temperature dependences of ^{3}He heat capacities in the 1D pores preplated by the ^{4}He film. They are described as $C = \beta_0 + \gamma T + \beta_2 T^2$. (b)–(d) Coverage n_3 dependences of β_0, γ, and $-\beta_2$, respectively.

state to the 2D state at the higher temperatures [18]. The calculation also indicates that the crossover peak disappears when T_F exceeds the gap temperature Δ/k_B. A heat capacity larger than $C/n_3R = 1$ at $T > 300$ mK is due to the 3D excitations to the E_{10} states and the higher states.

The calculated heat capacities in Fig. 2(b) reproduce the experimental results at the low coverages shown in Fig. 2(a), which show a characteristic peak or maximum at about 150 mK followed by approaching the magnitude of $C/n_3R \approx 1$ at the higher temperatures. The peak disappears with increasing the coverage. Therefore, the observed Schottky-like peak suggests a 1D-2D crossover around 150 mK.

To explore the lower-temperature state of the ^{3}He fluid in detail, the heat capacities below 50 mK are enlarged in Fig. 4(a). The temperature dependence can be fitted to an empirical formula, $C = \beta_0 + \gamma T + \beta_2 T^2$. In the present T range down to 5 mK, the γT term is dominant and is likely to correspond to the T-linear term of the degenerate Fermi gas or liquid. The coverage dependences of β_0, γ, and $-\beta_2$ are plotted in Figs. 4(b)–4(d), respectively. For the 1D ideal Fermi gas, the theoretical γ value decreases with increasing the density, because the density of states at the Fermi energy decreases as $1/\sqrt{\varepsilon_F}$ with increasing ε_F or the density. Although the lower two coverages, (●) and (○) in Fig. 4(a), satisfy the 1D condition for the ideal gas, the coverage (density) dependence of γ in Fig. 4(c) is inconsistent with that of the 1D Fermi gas. This arises from either some interaction in the 1D ^{3}He fluid or the deformation of $D(\varepsilon)$ in the actual 1D pore in the energy scale of a few tens mK. For example, a repulsive interaction is known to induce the same tendency of γ vs n_3 for the 1D Fermi gas [19]. A puddling effect of an attractive interaction may explain the increase of γ with n_3. Because the density of each puddle does not change, the increase of the puddle causes a variation of γ with n_3. As another possibility, if there is some heterogeneity in the potential along the 1D pore, the 1D density of state is deformed strongly from $1/\sqrt{\varepsilon}$ especially at the low energies. It may be caused by a small distribution of the pore diameter along the 1D pore. The variation of the ground state energy E_{00} of the transverse motion causes the changes of the energy ε and $D(\varepsilon)$ of the 1D gas.

In conclusion, we have produced a ^{3}He fluid by adsorbing ^{3}He on the ^{4}He-preplated 1D nanopores of FSM-16. Calculations of the heat capacity for a ^{3}He gas in the potential of the 1D nanopore reproduce the experimental Schottky-like peak around 150 mK followed by an approach to a 2D Boltzmann gas at the high T. The density dependence of the peak is consistent with this crossover model. The heat capacity below about 30 mK has a predominantly linear T dependence, which indicates the degenerate state of the 1D ^{3}He fluid. According to the calculation, the degenerate ^{3}He fluid at very low T is absolutely one dimensional in the sense that the azimuthal motion is confined to the ground state so that there remains only one motional freedom along the 1D pore.

The authors acknowledge D. S. Hirashima, M. Uwaha, and K. Miyake for valuable discussions about the Fermi degeneracy. This work was partly supported by a Grant-in-Aid for Scientific Research from the Ministry of Education, Science, Sports and Culture, Japan, and by the National Science Foundation, USA.

*Present Address: Department of Applied Physics and Chemistry, University of Electro-Communications, 1-5-1 Chofugaoka, Chofu, Tokyo 182-8585, Japan.
†Electronic address: nwada@cc.nagoya-u.ac.jp

[1] E. S. Hernández and J. Navarro, in *Microscopic Approaches to Quantum Liquids in Confined Geometries* edited by E. Krotscheck and J. Navarro (World Scientific, Singapore, 2002), p. 147.
[2] A. Casey, H. Patel, J. Nyéki, B. P. Cowan, and J. Saunders, Phys. Rev. Lett. **90**, 115301 (2003).
[3] N. Wada, A. Inoue, H. Yano, and K. Torii, Phys. Rev. B **52**, 1167 (1995).
[4] D. Ross, J. A. Phillips, J. E. Rutledge, and P. Taborek, J. Low Temp. Phys. **106**, 81 (1997).
[5] R. B. Hallock, Phys. Today **51**, No. 6, 30 (1998).
[6] N. Wada, H. Yano, M. Ogura, H. Namaizawa, and Y. Karaki, J. Low Temp. Phys. **110**, 357 (1998).
[7] N. Wada, H. Yano, and Y. Karaki, J. Low Temp. Phys. **113**, 317 (1998).
[8] N. Wada, J. Taniguchi, H. Ikegami, S. Inagaki, and Y. Fukushima, Phys. Rev. Lett. **86**, 4322 (2001).
[9] J. C. Lasjaunias, K. Biljaković, J. L. Sauvajol, and P. Monceau, Phys. Rev. Lett. **91**, 025901 (2003).
[10] S. Inagaki, Y. Fukushima, and K. Kuroda, J. Chem. Soc., Chem. Commun. 680 (1993).
[11] S. Inagaki, A. Koiwai, N. Suzuki, Y. Fukushima, and K. Kuroda, Bull. Chem. Soc. Jpn. **69**, 1449 (1996).
[12] J. Taniguchi, A. Yamaguchi, H. Ishimoto, H. Ikegami, and N. Wada, J. Low Temp. Phys. **134**, 595 (2004).
[13] H. Ikegami, T. Okuno, Y. Yamato, J. Taniguchi, N. Wada, S. Inagaki, and Y. Fukushima, Phys. Rev. B **68**, 092501 (2003).
[14] E. Cheng and M. W. Cole, Phys. Rev. B **38**, 987 (1988).
[15] E. S. Hernández, M. W. Cole, and M. Boninsegni, J. Low Temp. Phys. **134**, 309 (2004).
[16] L. Szybisz and M. Boninsegni, J. Low Temp. Phys. **134**, 327 (2004).
[17] M. Boninsegni, M. W. Cole, and F. Toigo, Phys. Rev. Lett. **83**, 2002 (1999).
[18] G. Stan and M. W. Cole, Surf. Sci. **395**, 280 (1998).
[19] T. Usuki, N. Kawakami, and A. Okiji, Phys. Lett. A **135**, 476 (1989).